

# Effect of Radiative Heat Transfer on Thermal Ignition

W. W. Yuen\* and S. H. Zhu†

University of California, Santa Barbara, Santa Barbara, California

The effect of radiative heat transfer on thermal ignition is analyzed numerically. Two specific problems are considered. They are 1) the "semi-infinite" problem in which a large mass of hot burnt gas is suddenly brought into contact with a large mass of cold unburnt air/fuel mixture, and 2) the "finite-hot-slab" problem in which a finite slab of hot burnt gas is suddenly immersed in a sea of cold unburnt air/fuel mixture. Numerical results show that in both problems the radiative emission and absorption by physical boundaries play essential roles in determining the effect of radiation on thermal ignition. In general, radiation is shown to have important effects on the ignition delay. For the finite-hot-slab problem, the minimum slab thickness required for ignition is also shown to depend strongly on the radiation effect. Both the optical thickness of the burnt mixture and the unburnt mixture are important in determining the actual effect of radiation.

## Nomenclature

$a$	= absorption coefficient, 1/m	$x_b(t)$	= coordinate of the foot of the flame, m
$B$	= dimensionless parameter, Eq. (11a)	$x_\delta(t)$	= half-thickness of the flame, m
$C$	= dimensionless parameter, Eq. (11b)	$\beta$	= dimensionless temperature ratio defined by Eq. (9)
$c$	= specific heat of gas, KJ/(Kg-K)	$\delta$	= dimensionless half-thickness of flame, $x_\delta/l_c$
$E_a$	= activation energy, KJ/Kmol	$\delta_0$	= value of $\delta$ at which $d\tau_m/d\theta = 0$
$E_n(x)$	= exponential integral function	$\delta_i$	= $\delta(\theta_c)$
$f(\eta)$	= dimensionless temperature profile, Eq. (21)	$\delta_{i,m}$	= minimum value of $\delta_i$
$F(\bar{n}, \lambda_c)$	= function utilized in Eq. (12)	$\epsilon$	= activation number, $E_a/R_c T_b$
$G_i (i = 1, 2, 3, 4, 5)$	= parameters defined by Eqs. (A3-A7)	$\zeta$	= dimensionless length defined by Eq. (2)
$I_i (i = 1, 2, 3, 4)$	= parameters utilized in Eqs. (22) and (23)	$\zeta_i$	= dimensionless initial position of the foot of the flame
$k$	= thermal conductivity of gas, W/(m-K)	$\zeta_{i,m}$	= minimum initial slab thickness for ignition
$K_u$	= initial optical thickness of the unburnt mixture	$\zeta_b(\tau)$	= dimensionless position of the foot of the flame
$K_b$	= initial optical thickness of the burnt mixture	$\zeta_L$	= dimensionless length of the one-dimensional system
$l_c$	= characteristic length defined by Eq. (3b), m	$\eta$	= dimensionless variable defined by Eq. (20)
$L$	= total length of the one-dimensional system defined in Fig. 1, m	$\theta$	= dimensionless time defined by Eq. (2)
$m$	= mass loading of the mixture, Kg/m <sup>3</sup>	$\theta_c$	= dimensionless time at which the two combustion zones are in contact
$M$	= dimensionless mass loading defined by Eq. (10)	$\kappa$	= optical thickness defined by Eq. (9)
$M_{bu}$	= mass loading ratio, $m_b/m_u$	$\kappa_{b-\eta}$	= optical thickness defined by Eq. (A8a)
$\bar{n}$	= complex index of refraction of particles	$\kappa_0$	= optical thickness defined by Eq. (A8b)
$N(\eta)$	= function defined by Eq. (A10)	$\kappa_{2\delta}$	= optical thickness defined by Eq. (A8c)
$q_r$	= radiative heat flux, W/m <sup>2</sup>	$\kappa_L$	= optical thickness defined by Eq. (A8d)
$\bar{q}_r$	= dimensionless radiative heat flux	$\lambda_c$	= characteristic wavelength, m
$\bar{Q}$	= volumetric heat generation rate, W/m <sup>3</sup>	$\rho$	= gas density, Kg/m <sup>3</sup>
$Q_0$	= characteristic heat of reaction, W/m <sup>3</sup>	$\sigma$	= Stefan-Boltzmann constant, W/(m <sup>2</sup> -K <sup>4</sup> )
$R$	= dimensionless heat generation rate defined by Eq. (4)	$\tau$	= dimensionless temperature defined by Eq. (2)
$\bar{R}$	= total dimensionless heat generation defined by Eq. (5)	$\tau_m$	= $\tau(0)$
$R_c$	= universal gas constant, KJ/(Kmol-K)	$\tau_{m,0}$	= value of $\tau_m$ at which $d\tau_m/d\theta = 0$
$S$	= dimensionless temperature gradient, $f'(0)$	$\phi(\tau)$	= dimensionless heat generation rate used in Eq. (1)
$t$	= time, s		
$t_c$	= characteristic time defined by Eq. (3a), s	<i>Subscripts</i>	
$T$	= temperature, K	$u$	= properties of the unburnt mixture
$x$	= space coordinate, m	$b$	= properties of the burnt mixture

Received Feb. 9, 1988; revision received June 23, 1988. Copyright © American Institute of Aeronautics and Astronautics, Inc., 1988. All rights reserved.

\*Professor, Department of Mechanical and Environmental Engineering, Member AIAA.

†Graduate Student, Department of Mechanical and Environmental Engineering.

## I. Introduction

THE present work is the second in a series of two papers that deals with the general effect of radiation on flame propagation and ignition. In the first paper<sup>1</sup> the effect of radiation on flame speed, flame thickness, and fuel consumption

rate (flame propagation parameters that are important after ignition has occurred) was demonstrated. The radiative properties of the combustion products and the reacting mixture, together with the radiation from the physical boundaries, were demonstrated to have significant effects on the flame propagation behavior. The present work considers the effect of radiative heat transfer on thermal ignition. Two specific one-dimensional problems will be analyzed. First, a large mass of hot burnt gas is suddenly brought into contact with a large mass of cold unburnt air/fuel mixture. The conditions under which ignition occurs and the magnitude of the ignition delay will be determined. Second, a slab of hot burnt gas is suddenly immersed in a sea of cold unburnt air/fuel mixture. The critical conditions required for ignition will be developed. Based on numerical results generated for the two cases, the fundamental effect of radiation (both from the medium and physical boundaries) on general ignition phenomena will be established.

In recent years, a number of works<sup>2-6</sup> have been reported dealing with the general effect of radiation on thermal ignition. For a one-dimensional planar absorbing-emitting homogeneous medium with volumetric Arrhenius heat generation, the critical ignition parameters (similar to that derived by Frank-Kamenetskii<sup>7</sup> in the no-radiation case) for thermal ignition are calculated by various numerical techniques or approximation procedures. In these analyses, the radiative heating (or cooling) of the medium by a hot (cold) wall was considered as the major physical mechanism leading to ignition (extinction). In many practical situations, however, the combustion in a premixed air/fuel mixture is promoted by the use of sparks or pilot flames. Ignition also can be induced by the simultaneous conductive and radiative heating of the premixed air/fuel mixture with a hot wall and hot combustion products. Even in an initially homogeneous air/fuel mixture, the heat generation is a function of the concentration of the reacting mixture and temperature. Results from the existing works<sup>2-6</sup> are clearly not applicable for such situations. The objective to the present work is to illustrate the effect of radiation on these important practical ignition problems.

**II. "Semi-Infinite" Problem**

The physical model is illustrated by Fig. 1a. A "large" slab of hot combustion products at temperature  $T_b$  is brought into contact with a large slab of cold unburnt air/fuel mixture at temperature  $T_u$ . The objective of the analysis is to determine conditions under which the energy generated by chemical reaction is sufficient to overcome thermal diffusion and ignite the unburnt mixture. As discussed in the previous work,<sup>1</sup> the assumption of a semi-infinite absorbing medium is accurate only in the optically thick limit. In order to illustrate the general effect of radiation for systems with arbitrary optical thickness, the analysis must include the existence of two black walls of temperature  $T_u$  and  $T_b$  in the considered one-dimensional system as shown in Fig. 1a.

As in the previous work,<sup>1</sup> the energy and species conservation equation can be simplified based on the Shvab-Zeldovich transformation and a procedure developed originally by Spalding<sup>8</sup> to become

$$\frac{\partial \tau}{\partial \theta} = \frac{\partial^2 \tau}{\partial \zeta^2} + \phi(\tau) - \frac{\partial \bar{q}_r}{\partial \zeta} \tag{1}$$

where  $\tau$ ,  $\theta$ , and  $\zeta$  are dimensionless temperature, time, and distance defined by

$$\tau = \frac{T - T_u}{T_b - T_u} \tag{2a}$$

$$\theta = \frac{t}{t_c} \tag{2b}$$

$$\zeta = \int_0^x \frac{\rho(x') dx'}{\rho_u l_c} \tag{2c}$$

The subscripts  $u$  and  $b$  stand for properties evaluated for the upstream unburned reacting mixtures ( $\tau = 0$ ) and the downstream burned products ( $\tau = 1$ ), respectively. Note that the region  $0 < \tau < 1$  can be interpreted physically as the combustion zone;  $t_c$  and  $l_c$  are the characteristic time and length given by

$$t_c = \frac{\rho_u c (T_b - T_u)}{Q_0 \bar{R}} \tag{3a}$$

$$l_c = \left[ \frac{k_u (T_b - T_u)}{Q_0 \bar{R}} \right]^{1/2} \tag{3b}$$

with  $Q_0$  being the characteristic heat of reaction and  $\bar{R}$  representing total dimensionless energy generation across the combustion zone. Mathematically, the dimensionless heat generation  $R$  is defined as

$$R = \frac{k(x) \dot{Q}(x)}{k_u Q_0} \tag{4}$$

with  $\dot{Q}$  being the volumetric heat generation rate and  $\bar{R}$  given by

$$\bar{R} = \int_0^1 R(\tau) d\tau \tag{5}$$

Physically,  $\bar{R}$  can be interpreted as the dimensionless heat generation across the reaction zone. As discussed in the previous work,<sup>1</sup> it is reasonable to assume, for many reactions, that  $R$  is only a function of the dimensionless temperature  $\tau$  given by

$$R(\tau) = (1 - \tau)^2 e^{-\epsilon/\tau} \tag{6}$$

with  $\epsilon = E_a/R_c T_b$  being the activation number. The source term  $\phi(\tau)$  in Eq. (1) is

$$\phi(\tau) = \frac{R(\tau)}{\bar{R}} \tag{7}$$

The radiative contribution to the energy balance is represented by the term  $\partial \bar{q}_r / \partial \zeta$  with  $\bar{q}_r = q_r / Q_0 \bar{R} l_c$  being the dimensionless radiative flux. For a one-dimensional gray absorbing and emitting medium (for example, a mixture of reacting gases and combustion products laden with small

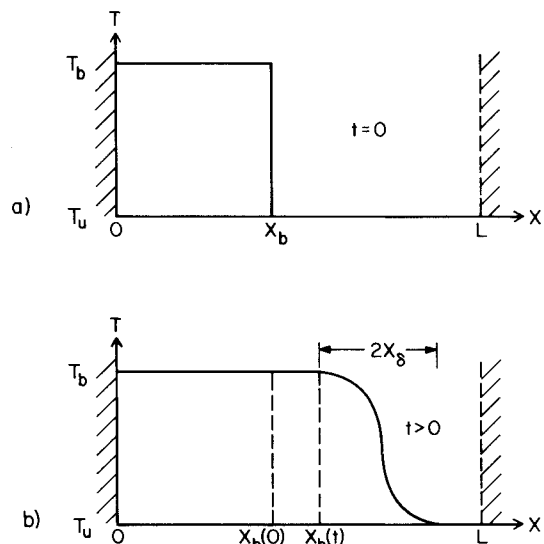


**Fig. 1** Geometry and expected temperature profile for the "semi-infinite" problem.

particles<sup>9</sup>),  $\bar{q}_r$  can be generated readily from the solution to the radiative transfer equation as

$$\bar{q}_r(\zeta) = 2\frac{B}{C}\left\{(1 + \beta)^4 E_3(\kappa) - \beta^4 E_3(\kappa_L - \kappa) + \int_0^\kappa [\tau(\kappa') + \beta]^4 E_2(\kappa' - \kappa) d\kappa' - \int_\kappa^{\kappa_L} [\tau(\kappa') + \beta]^4 E_2(\kappa' - \kappa) d\kappa'\right\} \quad (8)$$

with

$$\beta = \frac{T_u}{T_b - T_u}, \quad d\kappa = CM(\zeta) d\zeta \quad (9)$$

$$M(\zeta) = \frac{m(\zeta)}{m_u} \quad (10)$$

and  $B, C$  are dimensionless parameters given by

$$B = \frac{a_u \sigma (T_b - T_u)^4}{Q_0 \bar{R}} \quad (11a)$$

$$C = a_u l_c \quad (11b)$$

$$a_u = F(\bar{n}, \lambda_c) \rho_u m_u \quad (12)$$

Physically, small particles in the reacting mixture and products are assumed to be the primary species responsible for the radiative absorption and emission in the development of Eqs. (10-12);  $m(\zeta)$  represents the mass loading of the small particles. The dimensionless parameter  $B$  represents the ratio of radiative flux to reactive heat generation, while  $C$  stands for the optical thickness of the system based on the unburned absorption coefficient  $a_u$ . The two ends of the one-dimensional system are assumed to be bounded by black boundary at temperature  $T_u$  and  $T_b$ , respectively. The parameter  $F(\bar{n}, \lambda_c)$  is a function of the optical constant of the solid particles evaluated at a characteristic wavelength  $\lambda_c$ . The definition of various dimensional parameters are given in the Nomenclature section. A more detailed discussion of the physical assumptions and the mathematical development of the preceding equations were presented in the earlier work.<sup>1</sup> The initial condition, as represented by Fig. 1a, can be written as

$$\tau(\zeta) = \begin{cases} 1 & 0 \leq \zeta \leq \zeta_i \\ 0 & \zeta_i \leq \zeta \leq \zeta_L \end{cases} \quad (13)$$

with

$$\zeta_i = \frac{\rho_b x_b(0)}{\rho_u l_c} = \zeta_b(0) \quad (14a)$$

$$\zeta_L = \zeta_i + \frac{L - x_b(0)}{l_c} \quad (14b)$$

The solution to Eq. (1) subjected to the preceding initial condition can be generated readily by the integral method.<sup>1</sup>

If ignition occurs, the expected temperature distribution of the medium is illustrated qualitatively by Fig. 1b. The rate of movement of the foot of the flame,  $dx_b/dt$ , can be interpreted physically as the flame speed. Because of the thermal diffusion effect, numerical results show that  $dx_b/dt$  is always negative initially when the hot burnt mixture is brought into contact with the cold unburnt mixture. If ignition occurs,  $dx_b/dt$  must become positive at a later time, and the flame subsequently propagates forward. The time required for  $dx_b/dt$  to increase from its initial negative value to zero thus can be interpreted as the ignition delay.

Physically, the important radiation parameters are the initial optical thickness of the burnt mixture  $K_b$  and that of the unburnt mixture  $K_u$ , defined by

$$K_b = CM_{bu} \zeta_i \quad (15)$$

$$K_u = C(\zeta_L - \zeta_i) \quad (16)$$

Based on numerical results, the effect of the two optical thicknesses on the ignition delay  $\theta_i$  is illustrated by Fig. 2. The ignition delay for the no-radiation case is shown in the same figure for comparison.

Results in Fig. 2 illustrate readily that, in general, radiation always increases ignition delay because it enhances heat loss from the burnt mixture. In the limit of an optically thin burnt mixture, the radiative emission from the flame is small compared to conduction heat loss; the effect of radiation is thus insignificant. As the radiative emission from the flame becomes large ( $K_b = 0.2$ ), the ignition delay depends strongly on the optical thickness of the unburnt mixture. For cases with small  $K_u$ , the direct heat transfer between the flame and the cold boundary at  $\zeta = \zeta_L$  leads to a significant increase in the ignition delay. This corresponds physically to extinction. As  $K_u$  increases, the net radiative heat loss from the burnt mixture reduces, and the ignition delay decreases. In the limit of an optically thick unburnt mixture ( $K_u \rightarrow \infty$ ), the overall radiative heat loss from the flame is small. Independent of  $K_b$ , the effect of radiation leads simply to an increase in "effective" thermal conductivity, causing only a small increase in the ignition delay compared to the no-radiation case. Note that the case of a doubly infinite medium corresponds mathematically to the case with  $K_b = K_u = \infty$ . Such analysis would lead to an incorrect (but commonly assumed) conclusion that radiation produces essentially an added diffusion effect on the ignition delay. It is important to emphasize that a physically large system can be optically thin. The effect of radiative emission and absorption by the boundary must thus be included in any realistic analysis of the radiative heat-transfer effect.

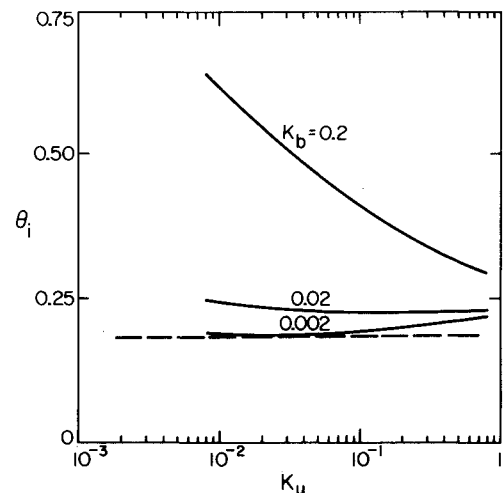


Fig. 2 Effect of optical thicknesses of the burnt and unburnt mixtures on the ignition delay for the semi-infinite problem (the broken line represents the no-radiation results).

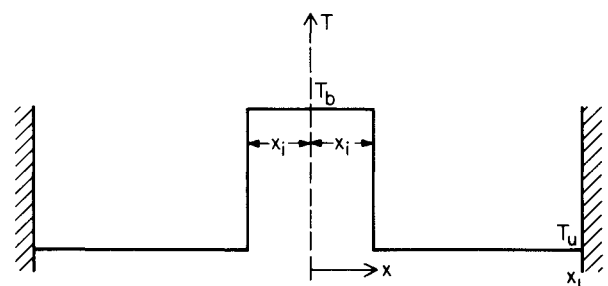


Fig. 3 Geometry and coordinate system for the "finite-slab" problem.

**III. "Finite-Hot-Slab" Problem**

The physical model is illustrated by Fig. 3. A slab of hot combustion products at temperature  $T_b$  and thickness  $2x_i$  is initially surrounded by a cold unburnt air/fuel mixture at temperature  $T_u$  on both sides. Because of the symmetry of the problem,  $x = 0$  is chosen to be the center of the initial hot slab, and the total thickness of the medium is taken to be  $2L$ . Using the same physical assumptions and definition of dimensionless variables as the semi-infinite problem, the dimensionless energy equation is again given by Eq. (1). Because of the change in coordinate system ( $\zeta$  is measured from the midpoint between the two walls, and  $\kappa_L$  now represents the optical thickness from the origin  $\zeta = 0$  to the wall at  $\zeta = \zeta_L$ ), the dimensionless radiative heat flux becomes

$$\bar{q}_r(\zeta) = 2\frac{B}{C} \left\{ \beta^4 [E_3(\kappa + \kappa_L) - E_3(\kappa_L - \kappa)] + \int_{\kappa_L}^{\kappa} [\tau(\kappa')] + \beta^4 E_2(\kappa' - \kappa) d\kappa' - \int_{\kappa}^{\kappa'} [\tau(\kappa') + \beta^4 E_2(\kappa' - \kappa) d\kappa'] \right\} \quad (17)$$

The initial condition, as represented by Fig. 3, is

$$\tau(\zeta) = \begin{cases} 1 & -\zeta_i \leq \zeta \leq \zeta_i \\ 0 & \zeta \leq -\zeta_i \end{cases} \quad (18)$$

For cases in which ignition occurs, the expected temperature profile after ignition is illustrated qualitatively by Fig. 4a. The transient flame propagating behavior is similar to that of the semi-infinite problem as presented in the previous work.<sup>1</sup> For the extinction and almost-ignition case, the expected temperature profile is shown qualitatively by Fig. 4b. The two combustion zones are in "contact," and the temperature at  $\zeta = 0$ ,  $\tau_m$  is less than 1.0. In the extinction case,  $\tau_m$  decreases monotonically toward zero after the initial contact. If ignition occurs, on the other hand,  $\tau_m$  will decrease to a minimum value greater than zero and, subsequently, increase. The medium will eventually achieve a temperature profile similar to that in Fig. 4a, and the flame will propagate. Since the objective of the present analysis is to determine the minimum slab thickness required for ignition, the present work will consider only the flame behavior after the initial contact of the two combustion zones. The integral method will be used to determine the behavior of  $\tau_m$  and  $\delta$ .

Specifically, assuming that the temperature profile has the following generalized form,

$$\tau(\zeta) = \begin{cases} \tau_m(\theta)f(\eta) & 0 \leq \zeta \leq 2\delta \\ 0 & 2\delta \leq \zeta \leq \zeta_L \end{cases} \quad (19)$$

where  $\eta$  is given by

$$\eta = \frac{\zeta - \delta}{\delta} \quad (20)$$

As demonstrated in Spalding<sup>8</sup> and solutions to the semi-infinite problem, numerical predictions for the ignition and flame propagation behavior are insensitive to the assumed dimensionless temperature profile  $f(\eta)$ . The same expression used in the previous work<sup>1</sup> is, thus, assumed to be applicable in the present case. It is

$$f(\eta) = 0.5 - \frac{1}{\pi} \tan^{-1} \left[ \frac{5.5\eta}{(1 - \eta^2)^4} \right] \quad (21)$$

Mathematically, Eq. (21) is generated by the combination of two "pieces" of error functions. Numerical experiments show that it is an adequate approximation of the temperature profile within the combustion zone. Note that  $\delta$ , in addition to being the dimensionless thickness of the combustion zone, can also be interpreted as the dimensionless flame center for the

present problem. Substituting Eq. (21) into Eq. (1), and integrating from 0 to  $\zeta_L$  and from  $\delta$  to  $\zeta_L$ , a set of two nonlinear ordinary differential equations can be generated for  $\delta(\theta)$  and  $\tau_m(\theta)$ . They are

$$\frac{d\delta}{d\theta} = \frac{2S}{\delta} + \frac{2}{\tau_m} \{ \delta [I_4 - I_2(I_3 + I_4)] - I_1 \bar{q}_r(\zeta_L) + \bar{q}_r(\delta) \} \quad (22)$$

$$\frac{d(\tau_m \delta)}{d\theta} = (I_3 + I_4)\delta - \bar{q}_r(\zeta_L) \quad (23)$$

with  $S = f'(0)$  being the dimensionless temperature gradient at  $\zeta = 0$ . The parameters  $I_1, I_2, I_3$ , and  $I_4$ , which are related to the integral of the dimensionless temperature profile and heat generation across the combustion zone, have been evaluated in the previous work.<sup>1</sup> Expressions for  $\bar{q}_r(\delta)$  and  $\bar{q}_r(\zeta_L)$  are given in detail in Appendix A. The initial condition for Eqs. (22) and (23) are

$$\tau_m(\theta_c) = 1.0, \quad \delta(\theta_c) = \delta_i \quad (24)$$

where  $\theta_c$  stands for the dimensionless time required by the initial step-function temperature profile (as shown in Fig. 3) to develop into a profile in which the two combustion zones are in contact (as shown in Fig. 4b);  $\theta_c$  and  $\delta_i$  (note that in general,  $\delta_i \neq \zeta_i$ ) can be determined from an "early time" solution to Eq. (1), which is equivalent to the semi-infinite case.

As in the semi-infinite problem, the important dimensionless parameters for the present problem are  $B, C, \epsilon, \zeta_i, \zeta_L, \beta$ , and the mass loading ratio  $M_{bu}$ . Physically, the parameter  $B$  illustrates the importance of the radiative effect relative to the chemical heat generation effect. The parameter  $C$  is a characteristic optical thickness that also represents the importance of the radiative effect compared to the conduction effect. Again, in contrast to previous ignition analyses that do not include the effect of radiation, the size and the optical thickness of the system (and the radiative emission and absorption by the two cold walls at  $\zeta_L$  and  $-\zeta_L$ ) play important roles in determining the effect of radiation on ignition.

To illustrate the mathematical behavior of  $\tau_m$ , it is useful to expand Eq. (23) and combine with Eq. (22) to yield

$$\frac{d\tau_m}{d\delta} = \frac{1}{\delta} \left\{ [(I_3 + I_4)\delta - \bar{q}_r(\zeta_L)] \left( \frac{d\delta}{d\theta} \right)^{-1} - \tau_m \right\} \quad (25)$$

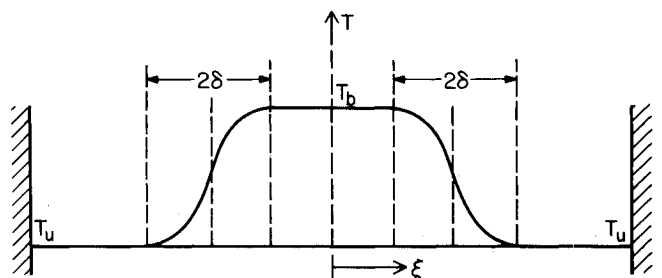


Fig. 4a Expected temperature profile for the finite-slab problem in which ignition occurs.

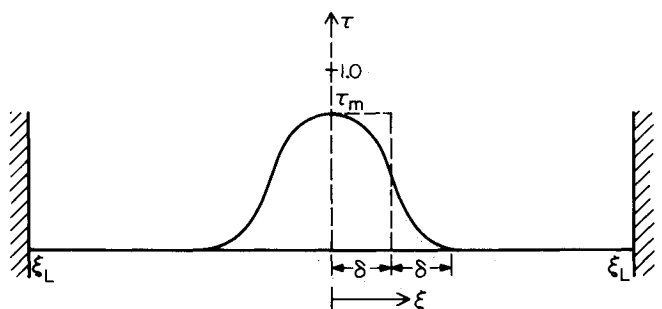


Fig. 4b Expected temperature profile for the finite-slab problem in which possible extinction occurs.

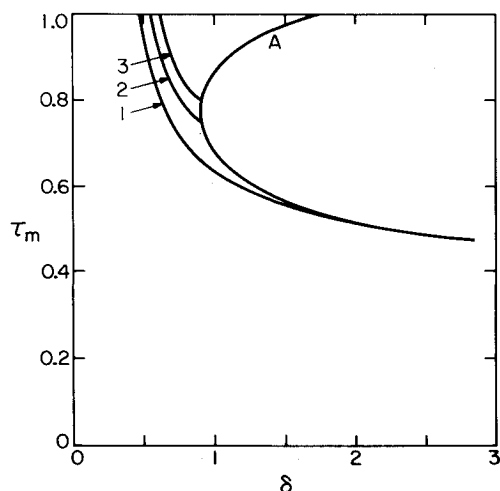


Fig. 5 Schematic representation of the numerical procedure used to determine the minimum ignition thickness. (Curve A represents the set of points at which  $d\tau_m/d\delta = 0$ . Curves 1, 2, and 3 represent the variation of  $\tau_m$  with  $\delta$  for various starting values of  $\delta$ . The starting value of  $\delta$  for curve 1 corresponds approximately to the minimum ignition thickness.)

Since  $d\delta/d\theta$  is always positive [as it can be observed readily from Eq. (22), and is also consistent with physical expectation], and  $d\tau_m/d\theta$  always starts out to be negative at  $\theta = \theta_c$  [as it can be observed readily from Eq. (23)],  $d\tau_m/d\delta$  is also negative at  $\theta = \theta_c$ . If ignition occurs,  $\tau_m$  must eventually increase back to 1.0. This requires a positive  $d\tau_m/d\delta$ . A necessary condition for ignition is, thus,  $d\tau_m/d\delta = 0$ . Mathematically, the smallest  $\zeta_i$  for which such condition can be satisfied will have the physical interpretation of a minimum ignition thickness.

Specifically, the following mathematical procedure is used to determine the minimum thickness required for ignition. For a given set of specified dimensionless parameters, a set of points  $(\tau_{m,0}, \delta_0)$  at which  $d\tau_m/d\delta = 0$  are first determined from Eq. (25). A typical set of solutions for  $(\tau_{m,0}, \delta_0)$  are illustrated in Fig. 5. For each set of  $(\tau_{m,0}, \delta_0)$ , Eqs. (22) and (23) are then solved (in backward time step) to determine the initial value of  $\delta_i$  [which is identical to  $\delta(\theta_c)$ ] at which  $\tau_m = 1.0$ . Some typical solutions for the  $(\tau_m, \delta)$  history generated from Eqs. (22) and (23) are also shown in Fig. 5 as illustrations. It can be observed readily [and also can be shown rigorously from Eqs. (22) and (23)] that as  $\delta_0$  increases, the corresponding  $\delta_i$  approaches asymptotically to a constant  $\delta_{i,m}$ . Mathematically, no solutions with  $\delta_i < \delta_{i,m}$  can achieve the condition of  $d\tau_m/d\delta = 0$ . When  $\delta_i < \delta_{i,m}$ , the centerline temperature  $\tau_m$  decreases monotonically to zero leading to extinction.

After  $\delta_{i,m}$  is determined, the early-time solution can be used to relate  $\delta_{i,m}$  to the minimum initial slab thickness  $\zeta_{i,m}$ . Numerical results, however, show that in all cases considered in the present work,  $\delta_{i,m}$  is essentially identical to  $\zeta_{i,m}$  (i.e., the flame does not move very much during the initial diffusion stage);  $\delta_{i,m}$  thus can be interpreted as the minimum hot-slab thickness required for ignition.

As in the previous work,<sup>1</sup> a survey of the physicochemical data and typical flame temperatures for common hydrocarbon fuels<sup>10</sup> suggests values of 5.0 and 10.72 for  $\epsilon$  and  $B/C$ , respectively. Numerical data for other values of  $\epsilon$  (which are of some practical interest in terms of analyzing different fuels and air/fuel ratios) are presented elsewhere.<sup>11</sup> Assuming that  $\zeta_L = 1500$ , the minimum ignition thicknesses for different absorption coefficients for the burnt mixture are calculated and presented in Fig. 6. The no-radiation result, which is identical to that generated by Spalding,<sup>8</sup> is presented in the same figure for comparison. The absorption coefficient of the unburnt mixture does not appear as a parameter in the figure because it has practically no effect on the minimum ignition thickness.

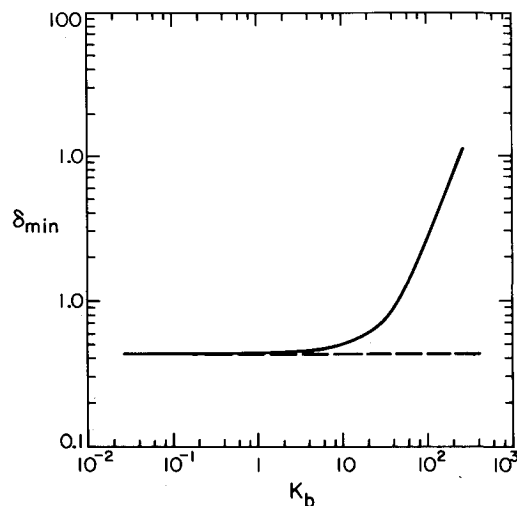


Fig. 6 Effect of the absorption coefficient of the burnt mixture on the minimum ignition thickness. The broken line represents the no-radiation result.

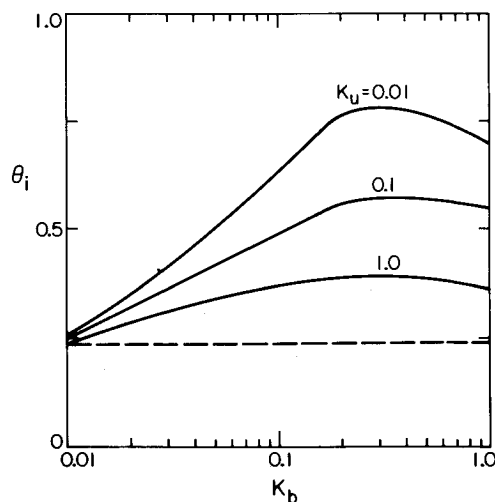


Fig. 7 Effects of optical thicknesses of the burnt and unburnt mixtures on the ignition delay for the finite-slab problem (the broken line represents the no-radiation results).

Physically, the major effect of radiation on the minimum ignition thickness is to increase the heat loss from the initial burnt mixture to the unburnt mixture and cold wall. As the optical thickness of the burnt mixture increases, the radiative heat loss increases, and a larger slab of burnt mixture is required for ignition. The lack of dependence on the optical property of the unburnt mixture suggests that the radiative heat transfer from the hot burnt mixture to the cold wall is the dominating cooling effect controlling ignition.

Another important physical result associated with the ignition process is the ignition delay. Assuming  $\zeta_i = 50$  (which is greater than the minimum ignition thickness calculated and presented in Fig. 6 and, therefore, the two-combustion zone does not meet, and ignition always occurs), results for the ignition delay are plotted for different initial optical thicknesses  $K_b$  and  $K_u$  in Fig. 7. Note that  $K_b$  and  $K_u$  are still defined by Eqs. (15) and (16). Although the optical properties of the unburnt mixture have only a small effect on the minimum ignition thickness, results in Fig. 7 show that its effect on the ignition delay is quite significant. Because of the increased preheating of the unburnt mixture by radiative absorption, the ignition delay decreases with increasing optical thickness of the unburnt mixture  $K_u$ . Increasing the optical thickness of the burnt mixture, on the other hand, first increases and then

decreases the ignition delay. Physically, the increase in the optical thickness of the burnt mixture leads to two competing effects on ignition delay. First, it increases the radiative heat loss from the burnt mixture and, second, it leads to additional preheating of the unburnt mixture. For a burnt mixture with small optical thickness, the first effect dominates, and the ignition delay thus increases with increasing optical thickness of the burnt mixture. In the limit of an optically thick burnt mixture, the increase in heat loss caused by an increase in optical thickness is small compared to the total energy radiated into the unburnt mixture by the burnt mixture. The second effect dominates and leads, therefore, to a reduction in ignition delay.

**IV. Conclusions**

An approximate analysis is performed to determine the ignition behavior of two simple problems: 1) a semi-infinite one-dimensional problem in which a slab of hot burnt mixture is brought into contact with a slab of cold unburnt air/fuel mixture, and 2) a finite-hot-slab problem in which a finite slab of hot burnt mixture is surrounded by a cold unburnt air/fuel mixture. In both cases, the present work can be considered as an extension of a previous work by Spalding<sup>8</sup> with the inclusion of the radiative heat transfer effect. The following conclusions are generated:

1) In general, the radiation effect increases ignition delay for both problems, and for the finite-hot-slab problem it increases the minimum thickness required for ignition. Physically, this is because of the heat-loss enhancement effect of radiation.

2) Radiative emission and absorption by physical boundaries play essential roles in determining the effect of radiation on ignition. Analyses that assume semi-infinite medium without boundary correspond only to cases with infinite optical thickness. Such analyses are thus not useful in illustrating the general effect of radiation.

3) For the semi-infinite problem, the ignition delay increases with the initial optical thickness of the burnt mixture. The optical thickness of the unburnt mixture has only minor effect on ignition delay, except in the limit of an optically thick burnt mixture. In the limit of an optical thick burnt mixture and an optically thin unburnt mixture, ignition fails.

4) For the finite-hot-slab problem, the minimum thickness required for ignition increases with increasing absorption coefficient for the hot burnt gas. The absorption coefficient of the unburnt mixture has practically no effect on the minimum ignition thickness.

5) When ignition occurs in the finite-hot-slab problem, the ignition delay depends on both the optical thickness of the hot burnt gas and of the cold unburnt mixture. The ignition delay decreases with increasing optical thickness of the unburnt mixture. For a fixed optical thickness of the cold unburnt mixture, increasing the optical thickness of the hot burnt gas first increases, and then decreases the ignition delay.

**Appendix**

Substituting Eq. (19) into Eq. (17) and evaluating at  $\zeta_L$  and  $\delta$ , one obtains

$$\begin{aligned} \bar{q}_r(\zeta_L) = & 2 \frac{B}{C} \beta^4 [E_3(\kappa_L + \kappa_{2\delta}) - E_3(\kappa_L - \kappa_{2\delta})] \\ & + 2B\delta(G_1 + G_2) \end{aligned} \tag{A1}$$

$$\begin{aligned} \bar{q}_r(\delta) = & 2 \frac{B}{C} \beta^4 [E_3(\kappa_0 + \kappa_{2\delta}) - E_3(\kappa_{2\delta} - \kappa_0)] \\ & + 2B\delta(G_3 + G_4 - G_5) \end{aligned} \tag{A2}$$

where

$$G_1 = \int_{-1}^1 \{ [1 - f(\eta)]\tau_m + \beta \}^4 E_2[\kappa_L + \kappa_{b-\eta}(-\eta)] N(\eta) d\eta \tag{A3}$$

$$G_2 = \int_{-1}^1 [\tau_m f(\eta) + \beta]^4 E_2[\kappa_L + \kappa_{b-\eta}(\eta)] M(\eta) d\eta \tag{A4}$$

$$G_3 = \int_{-1}^1 \{ [1 - f(\eta)]\tau_m + \beta \}^4 E_2[\kappa_0 + \kappa_{b-\eta}(-\eta)] N(\eta) d\eta \tag{A5}$$

$$G_4 = \int_{-1}^1 [\tau_m f(\eta) + \beta]^4 E_2[\kappa_0 + \kappa_{b-\eta}(\eta)] M(\eta) d\eta \tag{A6}$$

$$G_5 = \int_0^1 [\tau_m f(\eta) + \beta]^4 E_2[\kappa_{b-\eta}(\eta) - \kappa_0] M(\eta) d\eta \tag{A7}$$

with

$$\kappa_{b-\eta}(\eta) = C\delta \int_{-1}^{\eta} M(\eta') d\eta' \tag{A8a}$$

$$\kappa_0 = C\delta [1 + (M_{bu} - 1)\tau_m I_1] \tag{A8b}$$

$$\kappa_{2\delta} = C\delta [2 + (M_{bu} - 1)\tau_m] \tag{A8c}$$

$$\kappa_L = C[\zeta_L + (M_{bu} - 1)\tau_m \delta] \tag{A8d}$$

Physically,  $\kappa_0$  is the optical thickness from  $\zeta = 0$  to the flame center  $\zeta = \delta$ ;  $\kappa_L$  is the optical thickness of the half-domain ranging from  $\zeta = 0$  to  $\zeta = \zeta_L$ ;  $\kappa_{2\delta}$  is the optical thickness of the flame, and  $\kappa_{b-\eta}(\eta)$  stands for the optical thickness from  $\zeta = 0$  to an arbitrary  $\zeta$ . The functions  $M(\eta)$  and  $N(\eta)$  are given by

$$M(\eta) = 1 + (M_{bu} - 1)\tau_m f(\eta) \tag{A9}$$

$$N(\eta) = 1 + (M_{bu} - 1)[1 - \tau_m f(\eta)] \tag{A10}$$

**References**

<sup>1</sup>Yuen, W. W. and Zhu, S. H., "The Effect of Thermal Radiation on the Propagation of Laminar Flames," *Proceedings of the 8th International Heat Transfer Conference*, Vol. 2, 1986, pp. 835-842.  
<sup>2</sup>Khalil, H., Shultis, J. K., and Lester, T. W., "Stationary Thermal Ignition of Particle Suspensions," *ASME Transactions of the Journal of Heat Transfer*, Vol. 105, May 1983, pp. 288-294.  
<sup>3</sup>Arpaci, V. S., "Radiation Affected Thermal Ignition," American Society of Mechanical Engineers Paper 83-WA/HT-61, 1983.  
<sup>4</sup>Arpaci, V. S. and Tabaczynski, R. J., "Radiation-Affected Laminar Flame Quenching," *Combustion and Flames*, Vol. 57, 1984, pp. 169-178.  
<sup>5</sup>Arici, O., "Radiation Affect Thermal Ignition Near the Wall," *Fundamental and Applications of Radiation Heat Transfer*, HTD-Vol. 72, edited by A. M. Smith and T. F. Smith, American Society of Mechanical Engineers, New York, 1987, pp. 53-57.  
<sup>6</sup>Crosbie, A. L. and Pattabongse, M., "Radiative Ignition in a Planar Medium," *Journal of Quantitative Spectroscopy and Radiative Transfer*, Vol. 37, No. 2, 1987, pp. 192-203.  
<sup>7</sup>Frank-Kamenetskii, D. A., *Diffusion and Heat Transfer in Chemical Kinetics*, Plenum Press, 1969.  
<sup>8</sup>Spalding, D. B., "Approximate Solutions of Transient and Two-Dimensional Flame Phenomena: Constant-Enthalpy Flames," *Philosophical Transactions of the Royal Society of London*, Vol. 245A, 1957, pp. 352-372.  
<sup>9</sup>Yuen, W. W. and Tien, C. L., "A Simple Calculation Scheme for Luminous-Flame Emissivity," *The Sixteenth International Symposium on Combustion*, The Combustion Inst., Pittsburgh, PA, 1976, pp. 1481-1487.  
<sup>10</sup>Kanury, A. M., *Introduction to Combustion Phenomena*, Gordon and Breach Sciences Publisher, 1977.  
<sup>11</sup>Zhu, S. H., "A Study of the Effect of Thermal Radiation on Laminar Flame Propagation and Ignition," Ph.D. Thesis, Dept. of Mechanical and Environmental Engineering, Univ. of California, Santa Barbara, CA, 1986.